IEEE Access
Multidisciplinary | Rapid Review | Open Access Journal

Received April 25, 2018, accepted May 27, 2018, date of publication June 1, 2018, date of current version June 29, 2018.

Digital Object Identifier 10.1109/ACCESS.2018.2842749

YIG Thick Film as Substrate Overlay for Bandwidth Enhancement of Microstrip Patch Antenna

INTAN HELINA HASAN[1], (Member, IEEE), MOHD NIZAR HAMIDON[1,2], (Senior Member, IEEE), ALYANI ISMAIL[2], (Member, IEEE), ISMAYADI ISMAIL[1], ANWER SABAH MEKKI[1], MUHAMMAD ASNAWI MOHD KUSAIMI[1], SAMAN AZHARI[1], AND ROSIAH OSMAN[1], (Member, IEEE)

[1]Institute of Advanced Technology, Universiti Putra Malaysia, Seri Kembangan 43400, Malaysia
[2]Faculty of Engineering, Universiti Putra Malaysia, Seri Kembangan 43400, Malaysia

Corresponding author: Intan Helina Hasan (i_helina@upm.edu.my)

This work was supported in part by the Ministry of Science, Technology and Innovation, Malaysia (Science fund), under Grant 03-01-04-SF1860, Universiti Putra Malaysia (Putra) under Grant GP-I/9439400, and in part by the Ministry of Higher Education, Malaysia (NanoMITe), under Grant LRGS/2015/UKM-UPM/NanoMITe/04/02.

ABSTRACT Research on microstrip patch antenna (MPA) has been growing in the past few decades due to its planar profile and easy fabrication. Its simplicity of structure, which includes a conductive patch, a dielectric substrate, a ground plane, and a microstrip feeder, is making it more popular for integration in devices which are more focused on miniaturization and flexibility. There are, however, a few disadvantages of MPA, such as narrow bandwidth, low power, and limited inexpensive material selection if a current printed circuit board etching fabrication technique is used. Ferrite substrates are known to be able to help overcome this issue, but the properties of bulk ferrites are difficult to control. This paper aims to solve this problem by using thick-film technology, which utilizes a screen printing method to include ferrite thick film in the MPA structure as substrate overlay to help enhance the performance of MPA. Yttrium iron garnet was chosen as the starting ferrite nanopowders, and the preparation and characterization of the ferrite thick-film paste were carried out to investigate properties of the thick film. Results showed that the thick film showed moderate permittivity and permeability, which is suitable for MPA fabrication. The actual fabricated MPA with ferrite thick-film inclusion on FR4 substrate showed that the thick film improved the performance of MPA with low firing temperature of 200 °C. For MPA which is designed to work at 5.8 GHz, the return loss and −3-dB bandwidth improved 100% and 73%, respectively. In conclusion, ferrite thick-film inclusion in MPA fabrication has proven to improve the performance of the antenna in terms of return loss and bandwidth enhancement.

INDEX TERMS Ferrites, patch antennas, printed circuits, thick films, yttrium compounds.

I. INTRODUCTION

Antenna plays a very important role in telecommunication technology; without antenna integrated in a communication device, the device cannot send or receive information in the form of signals. There are several types of antennas, including dipole antenna, horn antenna, wire antenna and others. In 1950s, microstrip patch antenna (MPA) was first introduced [1] and since then has gained a lot of interests from telecommunication industry players due to its flat or planar profile, easy to fabricate, small size and lower manufacturing cost. This type of antenna is currently widely applied in wireless communication systems, including cellular devices, Global Positioning System (GPS) devices, and wireless internet routers [2], [3]. Patch antenna is typically constructed by fabricating a conductive patch onto a dielectric substrate. The permittivity and thickness of the substrate give influences to the parameters of the antenna, including the resonant frequency, bandwidth and return loss of the antenna [4], [5]. There are few types of materials that are being studied and used as the substrate, such as ceramic,

semiconductor, ferrimagnetic, synthetic and composite materials.

Ferrimagnetic materials or ferrites are one type of magnetic materials, having a certain degree of susceptibility to magnetization. However if compared to ferromagnetic materials, they have different magnetic ordering, thus they are weaker in terms of magnetization, and have incomplete or non-zero net magnetization. Based on these properties, ferrites are divided into two categories, which are hard and soft ferrites. Hard ferrites have high coercivity and high remanence after being magnetized, which makes them perfect as permanent magnets. Soft ferrites on the other hand, have low coercivity that makes the magnetic direction can be easily reversed to normal state with low loss energy. These types of ferrites also have high electrical resistivity and low magnetic losses at higher frequency range, which makes them suitable for microwave applications [6]. Ferrites are also being studied as substrates for patch antennas, which can be tuned when external magnetic field is applied [7]–[12].

The common fabrication processes for MPA are by printed circuit board (PCB) etching technology [13], or thick film technology which utilizes screen printing method [14]. The latter is preferred however due to its ease of fabrication, with less chemical handling. Thick film technology has been widely used in semiconductor production, either in surface mounted devices (SMT) fabrication or in printed film circuit (PFC) production. Another main advantage of this technique is that the material used for screen printing can be printed on any planar surfaces, from rigid to flexible substrates. This makes the thick film technology still relevant to the electronics industry nowadays, even though the technology has been around for decades.

Thick film technology is the next best solution for MPA fabrication, with ability to use various substrates and thick film pastes with different dielectric and electrical properties which can be tailored to suit the performance required. Nevertheless, it is difficult to control the parameters of the MPA if using conventional conductive thick film pastes alone such as silver paste or copper paste. Furthermore, the use of copper paste is not preferable due to its oxidization in air at room temperature. Ferrite substrates can help to improve the performance of MPA due to its moderately high permittivity and permeability, and also the anisotropic behavior of the materials [15]. Ferrite bulks have been considered for this purpose, however it is difficult to control the permittivity and permeability of the magnetic materials, and the fabricated ferrite substrates tend to be brittle, therefore these limitations become the reason of the bottleneck in research ferrites application in antenna fabrication.

This project proposed a novel ferrite thick film paste using nanosized ferrite powder and linseed oil based organic vehicle which have never been reported before. By utilizing thick film technology, microstrip patch antenna has been able to fabricate with improved performance using common FR4 substrate. Thick film technology also contributes in terms of ease of fabrication, with ability to screen print prepared thick film paste on any desired substrate.

II. YIG THICK FILM PASTE PREPARATION

For this work, yttrium iron garnet (YIG) nanopowders (CAS no. 12063-56-8, Sigma-Aldrich USA, <100nm particle size, 99.9% trace metals basis) were used as the active ferrite element for the thick film paste preparation. YIG is one type of garnet ferrites, which is also one type of soft ferrites. These types of ferrites do not retain magnetization when being demagnetized, as compared to hard ferrites [16]. They also have excellent properties such as high electrical resistivity, low magnetic anisotropy and low losses at microwave frequency [17]. For organic vehicle, linseed stand oil (CAS no. 67746-08-1, Daler-Rowney) was used as the main ingredient due to its ability to polymerize even under room temperature. Linseed oil is often used as drying oil in paintings since it has boiling point of 346°C, making it suitable to be used for lower firing temperature. Linseed stand oil has higher viscosity compared to raw linseed oil, therefore it has been chosen as the organic binder for the thick film paste. M-xylene (CAS no. 108-38-3, Sigma-Aldrich USA, ReagentPlus grade, 99% assay) and α-terpineol (CAS no. 10482-56-1, Sigma-Aldrich USA, natural, $\geq$96% assay) were added as solvents for the organic vehicle.

In the paste preparation process, the organic vehicle was first prepared by mixing 85 wt% linseed stand oil with 12.5 wt% m-xylene using magnetic stirrer at 250 rpm for 3 hours, and later 2.5 wt% α-terpineol was added to the mixture which was then continued stirring for another 2 hours. During the mixing process, the temperature was kept at 40°C. The weight ratio of the components of the organic vehicle was based on the previous study carried out by Abadi [18]. Next, the prepared organic vehicle was added to ferrite nanopowder with optimized powder to organic vehicle weight ratio based on previous study [19], mixed thoroughly using sonicator for 1 hour with 10 minutes interval after 30 minutes to obtain homogenous paste for thick film printing. At this stage, sonicator was chosen to mix and disperse the powders due to magnetic behavior of the nanopowders used for thick film paste which makes the magnetic stirrer not suitable for mixing purpose.

The paste was then characterized to observe the viscosity and rheology properties of the ferrite paste using rheometer (Anton-Paar Rheoplus MCR301). There were two measurement conditions studied, which were relationship of viscosity and time with shear rate fixed at 100 s^{-1}, and observation of viscosity change when subjected to increased shear rate from 0.1s^{-1} until 1000 s^{-1}. Next, the thermal analysis was carried out using thermal gravimetric analysis (TGA) (Mettler Toledo TGA/DSC 1 HT) to study effect of firing temperature to the paste composition. For firing temperature analysis, the samples were put into aluminum crucible and set into TGA system with temperature sweep from 30°C to 500°C in nitrogen gas atmosphere.

III. THICK FILM CHARACTERIZATION

The prepared thick film paste was then printed onto alumina substrate using screen printing method for characterization purpose, as shown in Fig. 1. The thick film was printed using a silk screen frame with a certain design, preferably a square or rectangle area, using a screen printing machine. Next, the prepared sample was dried first at temperature 100°C for ten minutes, and later fired at temperature of 200°C and 300°C for 30 minutes in a box furnace (HT4–1600–SIC, Malaysia) to observe printability of paste to the substrate according to different firing temperature.

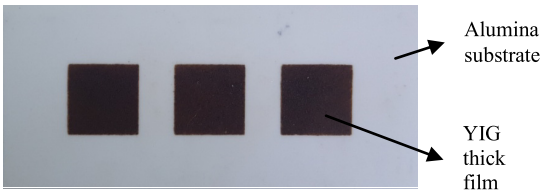

FIGURE 1. Screen printed ferrite thick film for characterization.

After the paste was printed onto selected substrate, the thick film samples were then characterized for structural morphology using Field Emission Scanning Electron Microscope (FESEM) (Hitachi S-3400N), while elemental analysis to determine composition of the paste was done using energy dispersive x-ray (EDX) analysis. To prevent charging of the materials, the samples were coated with gold using sputter coater first before being put onto the sample holder.

Permittivity and permeability of the samples were measured using Impedance Analyzer (Agilent HP4291B) for frequency ranging from 10MHz to 1GHz. The thick film paste samples were dried in molded clay to produce pellet-like thick film without substrate, with the thickness of the samples were from 5mm to 7mm. Then, the samples were tested first for permittivity, and later for permeability where the samples were cut according to the size and dimension of the sample holder. Apart from permittivity and permeability, the impedance analyzer was also used to measure the dielectric loss tangent. The magnetic properties were also observed using vibrating sample magnetometer (VSM) (Lakeshore 7404) of which thick film samples was cut to maximum measurement size which is 4mm × 4mm.

IV. MICROSTRIP PATCH ANTENNA FABRICATION

Before fabrication was performed, simulation was first needed to design the patch antenna according to specified or targeted parameters. For this project, the antenna was designed to work in frequency 5.8GHz, which can be used for WiFi application. The simulation was carried out using Computer simulation technology (CST) Studio Suite software, commonly utilized to design antennas. The simulation was carried out by using FR4 substrate which includes a copper layer on one side that works as the ground plane. After the designs were completed, they were then transferred to Adobe Illustrator software to prepare design suitable for stencil screen preparation. Stencil screen was then prepared by silk screen supplier (Khai Lien Silk Screen Supplies Sdn. Bhd.) which included artwork preparation, stretching, etching and exposing.

After thick film characterization was completed and suitable thick film parameters were determined, fabrication of microstrip patch antenna was done by first printing ferrite thick film onto FR4 substrate. After the thick film was dried and fired at 200°C for 30 minutes to ensure adhesion, a conductive patch and microstrip transmission line using silver paste was then screen printed onto the thick film layer to form a radiating patch for the antenna, and afterwards dried and fired using the recommended firing temperature in the specification sheet, which is 150°C for 30 minutes to obtain optimum conductivity. Afterwards, the patch antenna was cut to the specific dimension according to the simulation being done previously. A SubMiniature version A (SMA) connector is then soldered or adhered to the patch antenna for measurement preparation.

Finally, after fabrication of the antenna was completed, the return loss and resonant frequency for all prepared samples with different parameters were measured using Vector Network Analyzer (VNA) (Keysight, PNA 5227A). The measurement frequency range was set between 4GHz up until 8GHz. The fabricated patch antenna with an SMA connector fixed at the feeding point was connected to a cable which was linked to S1 port. The measurement taken for this project was basically S11 parameters, which refers to the value of power being reflected back to S1 port. A comparison was made between patch antenna with and without ferrite thick film to observe frequency shift, return loss and antenna bandwidth to confirm the performance of the ferrite thick film patch antenna.

V. RESULTS AND DISCUSSION

A. RHEOLOGY

Fig. 2 shows the viscosity of YIG paste versus time at shear rate fixed at 100 s^{-1}. The measurement was carried out for

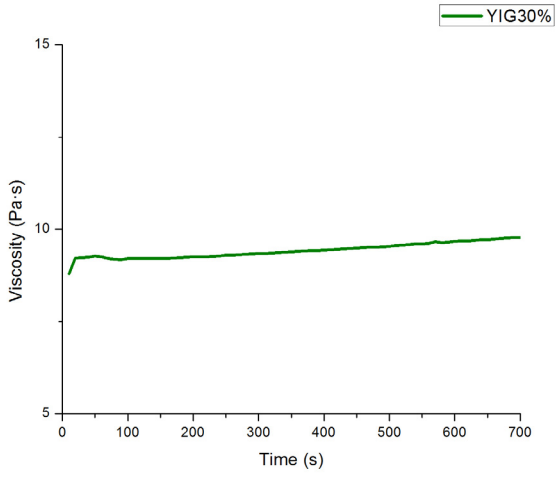

FIGURE 2. Viscosity vs. time measurement of YIG thick film paste.

10 minutes to observe changes in viscosity over a long period of time. It can be observed from the graphs that all samples showed steady increase in viscosity. It can be observed that the viscosity did not increased much, indicating the stability of the paste viscosity over time. This is also important characteristics of the paste, since during printing, it is preferable to have paste that does not dry off too quickly when it is being set onto the silk screen frame and before it is being squeezed through the mesh.

During screen printing process, different steps of the printing requires various shear rate. For example, when the paste is going through the opening mesh of the frame, the shear rate can be as high as 980 s^{-1} [20]. Therefore, it is important to understand the viscosity changes in the thick film paste when subjected to different shear rates. Fig. 3 shows the viscosity versus shear rate from 0.1 s^{-1} to 1000 s^{-1} to observe trend of viscosity with increase of the shear rate. Viscosity of YIG paste showed steady decrease throughout the measurement, which started with high viscosity and then decreased slowly when reaching 500 s^{-1}, and afterwards decreased sharply towards 1000 s-1. Therefore it can be concluded that pastes with weight ratio of 30% are most suitable for thick film fabrication due to their rheology properties, especially the viscosity change when subjected to high shear rate, which means that when the paste is at the point of penetrating the screen mesh, lower viscosity can help the paste to flow easily through the mesh and enable good printed thick film on the substrate, and when the printing is done, the viscosity returns to high value which can prevent bleeding or smearing of the paste.

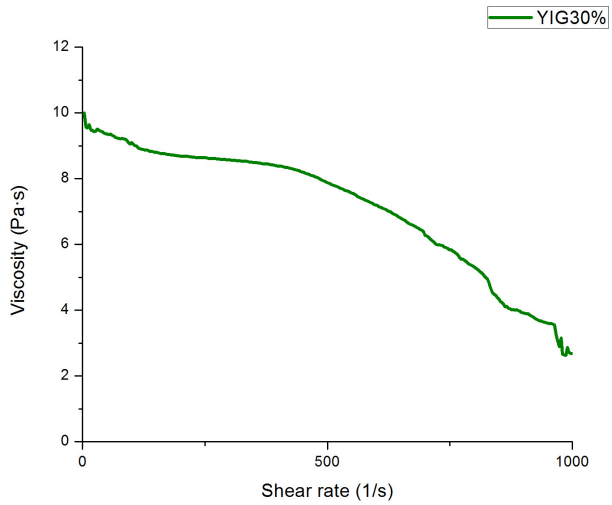

FIGURE 3. Viscosity vs. shear rate measurement of YIG thick film paste.

B. THERMAL PROPERTIES

In order to understand the effect of firing profile, specifically firing temperature and firing time of the thick film paste, TGA measurement was carried out to the sample. Fig. 4 shows the weight loss percentage and decomposition

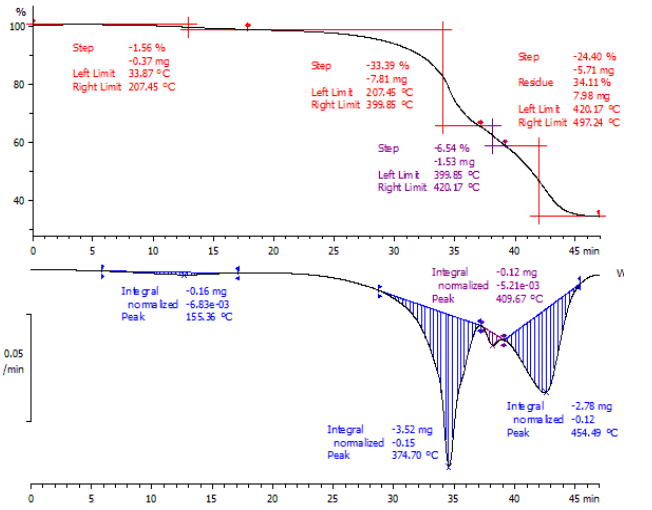

FIGURE 4. TGA measurement of YIG thick film paste.

rate for temperature ranging from 30°C to 500°C for YIG thick film paste under nitrogen atmosphere. Meanwhile, the TGA result of linseed stand oil is shown in Fig. 5 for comparison.

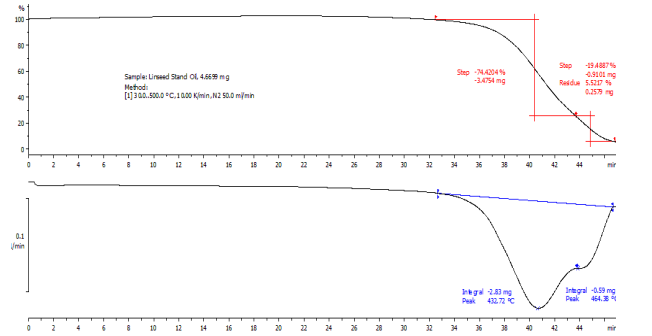

FIGURE 5. TGA measurement of linseed stand oil.

The volatile phase of the paste evaporated starting from 50 to 270°C, of which correlates with flash point and boiling point of m-xylene (flash point: 25°C, boiling point: 138°C) and α-terpineol (flash point: 90°C, boiling point: 217°C), respectively. Next phase was the removal of non-volatile material of organic vehicle which is the linseed stand oil, which has flash point of 200°C and boiling point from 300°C, according to specification sheets of the materials. It can be observed that the boiling phase of linseed oil peaked at 376°C. Finally, from 400°C to 500°C, decomposition occurred again which is related to linseed oil decomposition, since at this point, almost all organic vehicle had been evaporated and decomposed, leaving the ferrite powders on the substrate. Therefore, it can be concluded that the temperature suitable for the ferrite thick film with linseed oil as organic vehicle is from 200°C to 300°C, which makes the linseed oil base organic vehicle suitable for thick film designed with low firing temperature.

C. SURFACE MORPHOLOGY

The effect of firing temperature to the surface morphology of the thick film is further investigated. There were four samples with different firing temperature chosen for observation, which were samples left at room temperature, during drying process at 100°C, firing temperature of 200°C and firing temperature of 300°C. Fig. 6 and Fig. 7 show the FESEM images and EDX analysis of YIG thick films fired at these different temperatures.

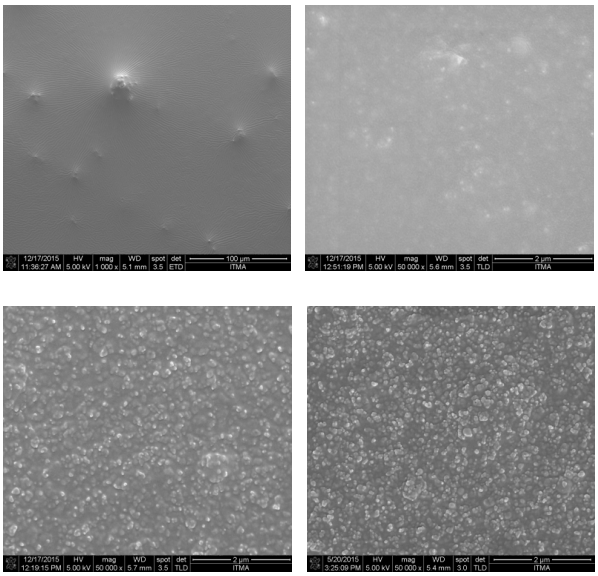

FIGURE 6. FESEM images of YIG thick film fired at different firing temperatures.

From the images, it can be observed that at room temperature, the organic vehicle was not dried off yet, indicating that the surface is still covered with the organic vehicle which is linseed oil-based. When the temperature is increased to 100°C, the organic vehicle started to dry but not enough to make the nanoparticles visible on the surface. At firing temperature of 200°C, the particles started to be visible, although the dispersion was not as clearly seen as the image for firing temperature of 300°C, of which the nanoparticles is clearly visible, as well as the dispersion of the powders. EDX analysis of all samples also confirmed the effect of firing temperature, of which the carbon element found in the organic vehicle to be decreased, while other elements associated YIG started to increase with the increase of the firing temperature. The EDX results implied that with increase in temperature, the organic vehicle which mainly consists of linseed oil evaporated or dried off from the surface, revealing the nanoparticles underneath the oil layer.

In conclusion, samples with 200°C and 300°C showed good visibility of the nanoparticles on the surface of the thick film, which can have effect on the properties and performance of the thick film. However there is no significant change in grain growth or phase change of the starting materials due to the low firing temperature used, which showed that the firing temperature did not give effect to the microstructure of

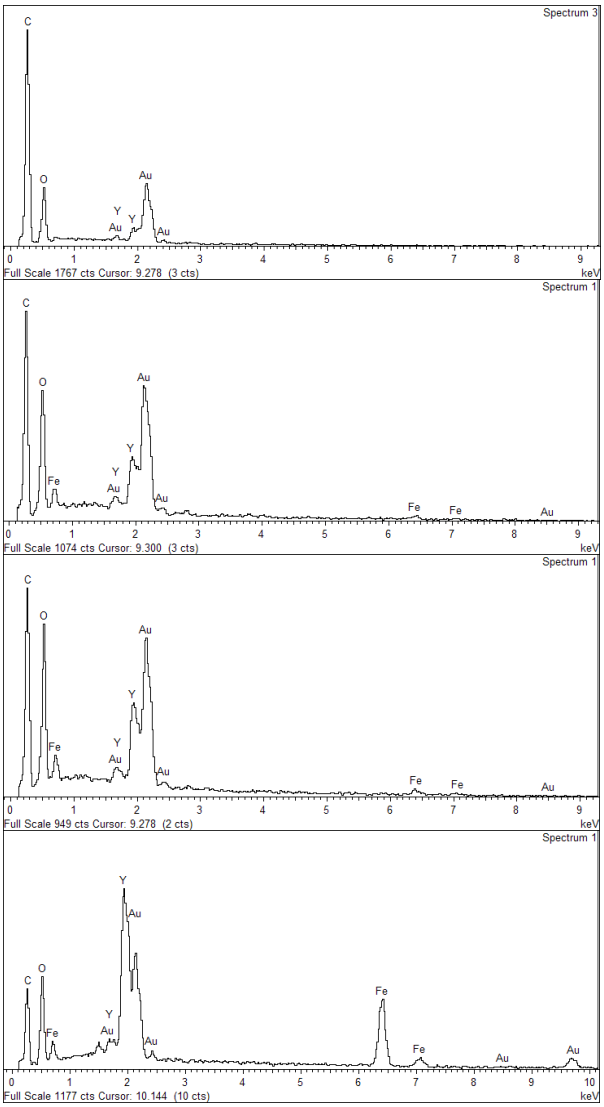

FIGURE 7. EDX analysis of YIG thick film fired at different firing temperatures.

the materials used, and this is favorable to those researchers who prefer not to have their materials changed in terms of microstructure or phase change [17]. Therefore, both firing temperatures can be used as firing temperature for thick film fabrication, depending on the maximum temperature limit of the chosen substrate for fabrication.

Finally, YIG thick film was observed from the cross-sectional images to study the adhesion, thickness and dispersion of the thick film paste onto the substrate. Fig. 8 shows the FESEM images of YIG thick film from the cross-sectional view to study the adhesion, thickness and dispersion of the thick film paste onto the substrate. YIG thick film showed good homogeneity with very few voids, and a very smooth surface, showing good dispersion of the nanoparticles. The thick film also showed excellent adhesion with the substrate. The thickness of YIG thick film calculated from the cross-sectional image is approximately 20um, which is acceptable thickness for thick film.

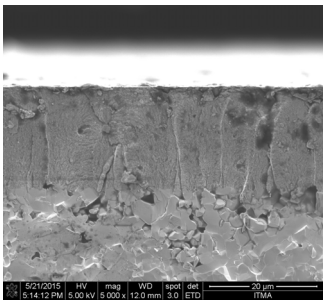

FIGURE 8. Cross-sectional image of YIG thick film on alumina substrate.

D. DIELECTRIC AND MAGNETIC PROPERTIES

The performance of a microstrip patch antenna relies heavily on the dielectric properties of the substrate of the antenna, as being highlighted in the introduction. Therefore, the dielectric properties of the ferrite thick film which acts as an overlay to the conventional substrates of the antenna is one of the main important properties that needs to be studied and analyzed. Dielectric properties of the thick film include the permittivity, or sometimes called dielectric constant of the thick film; and dielectric loss tangent; of which both can be measured using impedance analyzer. Meanwhile, ferrites are magnetic materials with ferrimagnetic behaviours, therefore the magnetic properties also need to be investigated to understand how or if the behaviours can have effect on the performance of antenna. The magnetic properties studied or measured in the work include permeability and hysteresis curve of YIG.

1) PERMITTIVITY

Fig. 9 shows the real permittivity of YIG thick film for frequencies ranging from 10MHz to 1GHz. From the graph, YIG thick film has permittivity of ($\varepsilon' = 4.29$) at frequency of 1GHz, and the value remained consistent throughout the frequency measured, except below 100MHz of which the permittivity seemed to decreased significantly from the initial permittivity. These results are compared with the findings by other researchers [21], [22]. For YIG thick film, the permittivity reported was around 14 to 15, higher than current results. The explanation for this variance may be due to the YIG powder ratio of the thick film. The result reported by [23] mentioned that the permittivity of YIG is 14.4, of which the sample is pure YIG nanopowders molded to a sample holder with thick of 0.5mm. Therefore, our results are acceptable of which the weight ratio of YIG powder in the thick film paste is only 30% wt.

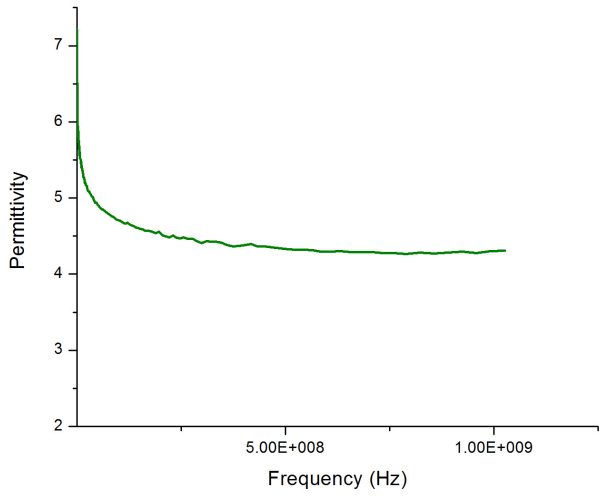

FIGURE 9. Real permittivity of YIG thick film.

YIG has a complex structure, with a total of 160 atoms with a unit cell that has eight formula units, with Fe^{3+} ions occupying inequivalent positions at octahedral and tetrahedral sites. Therefore a large number of Fe ions contribute to the high permittivity of YIG [24].

2) DIELECTRIC LOSS TANGENT

Fig. 10 shows the dielectric loss tangent (tan δ) of the YIG thick film. The value of the loss tangent, which is also referred to as the dissipation factor (D_f), is 0.05 for YIG thick film. This value is slightly higher than typical FR4 substrate which varies from 0.03 to 0.04, but nevertheless the thick film can be considered as low loss materials, which is suitable for antenna fabrication. From the graph, it can also be anticipated that the value remained almost constant with not much difference for frequencies higher than 1GHz, as shown and proved by [21].

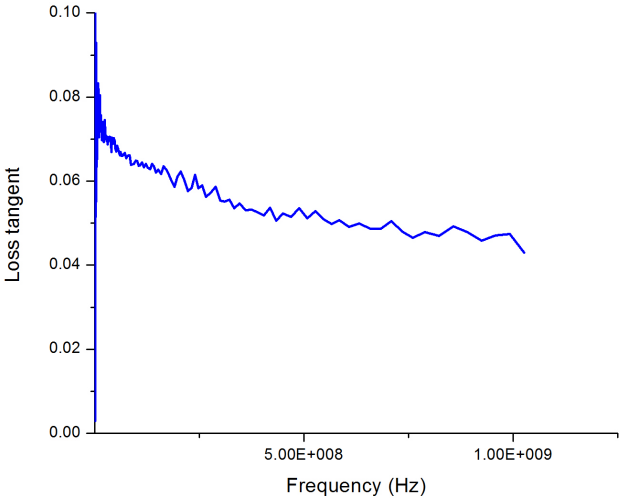

FIGURE 10. Dielectric loss tangent of YIG thick film.

Based on the graph, dielectric loss of YIG thick film decreased when frequency is increased, which is related to the behaviour of spinel ferrites. One of the reasons is that when a certain frequency is reached, the electronic exchange between ferrous ions cannot follow the alternating field anymore. Another possible reason is the strong correlation between dielectric constant and conduction mechanism of ferrites. Conduction mechanism refers to hopping of electrons from

Fe^{2+} to Fe^{3+}, therefore when the hopping frequency is equal to the external field, the maximum losses can be observed.

3) PERMEABILITY

Fig. 11 shows the real permeabilty of YIG thick film. At 1 GHz, the real permeability of YIG thick film is 0.868, which confirmed the theory that after 600MHz, the permeability remains constant at 1 [21], [23]. Furthermore, the content of YIG in thick film is relatively small, which is 30 wt%, which makes it less permeable than typical bulk ferrites.

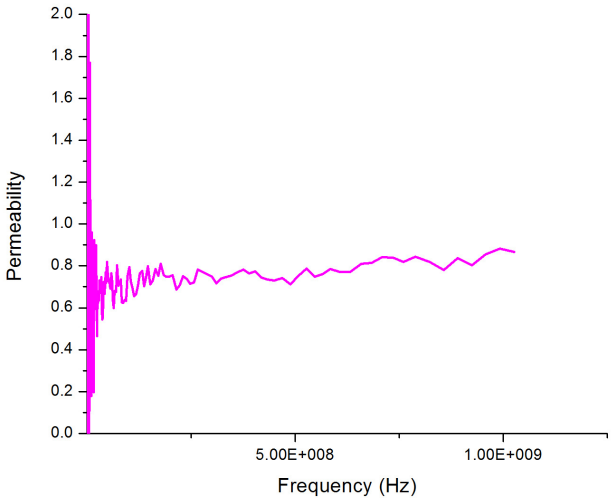

FIGURE 11. Real permeability of YIG thick film.

The low permeability of the thick film also agrees with explanation by [21], which also did research on the ferrite-polymer thick film composites. According to Verma, due to the presence of non magnetic material in the thick film, in this case the organic vehicle, the thick film is expected to have low permeability since the organic vehicle which surrounds the ferrites nanoparticles makes the ferrites have discontinuity in terms of magnetic flux. According to Snoek's rule, low permeability leads to higher resonance frequency of the material, therefore it is expected that the thick film has high resonance frequency compared to bulk ferrites. The thick film also shows very low loss factor, as shown in Fig. 12. The results are also in agreement with the findings reported in [22], of which the loss factor for nanosized ferrites are consistently low at high frequency range.

4) HYSTERESIS CURVE

Next, the hysteresis curve of both YIG thick film is studied. From the hysteresis curve, or sometimes referred to as M-H curve or M-H loop, other important values such as saturation magnetization, remanence or retentivity, and coercivity can be obtained. Fig. 13 shows the hysteresis curve of YIG thick film, with the inset graph showing the hysteresis for YIG in powder form. The saturation magnetization of YIG thick film is $Ms = 0.125 \times 10^{-3}$ emu/cm^3 or $4\pi Ms = 1.571 \times 10^{-3}$ G which is very low compared

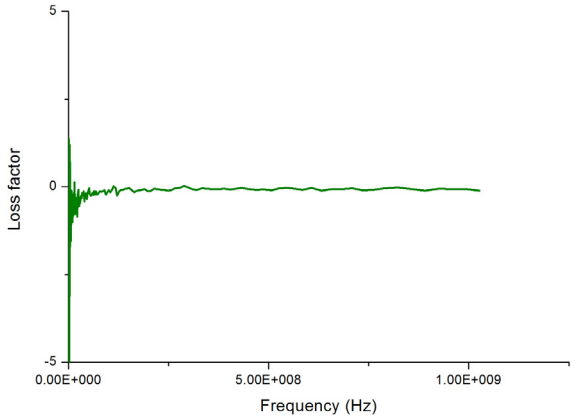

FIGURE 12. Loss factor of YIG thick film.

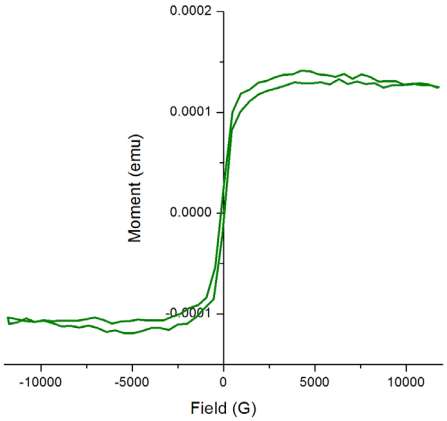

FIGURE 13. Hysteresis curve of YIG thick film.

with YIG powder, which has the value of 1.01×10^{-3} emu/cm^3 or $4\pi Ms = 12.692 \times 10^{-3}$ G. This shows that YIG thick film has very weak magnetization due to low magnetic mass related to weight ratio of YIG in thick film. The retentivity for YIG thick film also shows same pattern, proving that for YIG thick film, the material is very weak to retain the magnetization YIG powders. As for coercivity, both materials show weak coercive force, of which this agrees to properties of soft magnets. Meanwhile, previous study [25] shows that the resonance linewidth (ΔH) of YIG is 1.16 Oe.

E. MPA SIMULATION

Before MPA fabrication, simulation was carried out to determine the design and the dimension of the patch and the substrate. A minor change in the dimensions can have great effect in the parameters of the MPA. Therefore, simulation of the MPA is one crucial step before the fabrication. As mentioned in the scope of the project, the resonant frequency of the MPA is set to 5.8GHz, the frequency of a WiFi band according to ITU regulations. For fabrication, FR4 substrate was chosen for study in this work. The simulation was done with only silver paste as the radiating patch to fix the dimensions of the substrate and patch regardless of the ferrite thick film properties.

The thickness of radiating patch, t, and height of substrate, h, is usually smaller than the wavelength. The width of the patch, W, can be calculated by

$$W = \frac{v_o}{2f_r}\sqrt{\frac{2}{\varepsilon_r + 1}} \quad (1)$$

where v_0 is the free-space velocity of light, and f_r is the resonant frequency.

The length of the patch, L, is usually half of the wavelength. In order to calculate the physical length however, the fringing fields at the edges of the patch must be taken into account since they make the electrical length larger than the physical length of the patch. The fields are fringing due to finite length and width of the patch when it is charged through the transmission line.

Since the fringing fields travel through air and the substrate, effective dielectric permittivity or ε_{reff} is introduced to take into account the fields and propagation in the line. ε_{reff} can be calculated by

$$\varepsilon_{reff} = \frac{\varepsilon_r + 1}{2} + \frac{\varepsilon_r - 1}{2}\left[1 + 12\frac{h}{W}\right]^{-0.5} \quad (2)$$

The extension of the length, ΔL can be calculated by

$$\Delta L = 0.412h\frac{\left(\varepsilon_{reff} + 0.3\right)\left(\frac{W}{h} + 0.264\right)}{\left(\varepsilon_{reff} - 0.258\right)\left(\frac{W}{h} + 0.8\right)} \quad (3)$$

Then the actual patch length can now be calculated by

$$L = \frac{v_o}{2f_r\sqrt{\varepsilon_{reff}}} - 2\Delta L \quad (4)$$

Based on the calculations using equations (1) – (4), and substrate dimension calculations by [26], the dimensions of the MPA required for simulation purpose as well as the parameters of the FR4 substrate used are obtained. The relative permittivity of FR4 substrate is 4.3, with thickness of 1.57mm, and the ground plane for substrate is made from copper, with thickness of 0.035mm.

After all parameters were calculated, next step is to input all the dimensions in the CST Studio Suite software and run the simulation to determine the simulated resonant frequency. After the initial simulation, optimization were done later using parameter sweep function in the simulation software to determine the most optimized values for the MPA design. By using parameter sweep, all the dimensions can be set to variable numbers and each dimension can be simulated with the pre-determined values. The significant difference between theoretical calculations and simulation results is due to big amount of other input information used in the simulations, including conductivity of the conductive material, loss tangent of the dielectric substrate, and matching impedance of the microstrip feeder. Table 1 shows comparison between theoretical dimensions and simulation results of MPA dimensions.

Fig. 14 shows simulation result of MPA with FR4 substrate after optimization using parameter sweep function.

TABLE 1. Dimensions values of substrate and patch of MPA.

Item	Theoretical value	Simulation value
Relative permittivity, ε_r	4.3	4.3
Thickness, h (mm)	1.57	1.57
Length of patch, Lp (mm)	11.2	11.4
Width of patch, Wp (mm)	15.9	15.0
Length of substrate, Ls (mm)	20.6	25.0
Width of substrate, Ws (mm)	25.3	20.0
Width of microstrip feeder, Wf (mm)	3.0	1.0

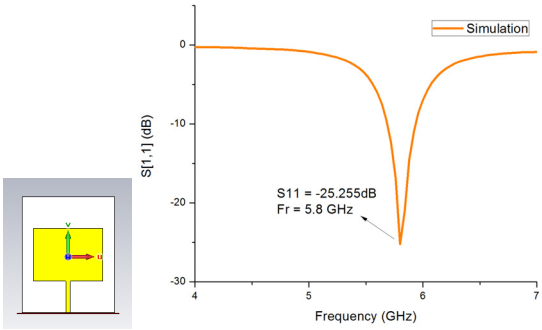

FIGURE 14. Simulation result of MPA with FR4 substrate at 5.8GHz.

For simulation of MPA using FR4 as substrate, the resonant frequency obtained after optimization is 5.8GHz, with S_{11} at −25.255 dB. Based on the simulation results, for dimensions of the radiating patch, there was not much difference from the theoretical calculations. However, for the dimensions of the FR4 substrate, it was found that after parameter sweep was done to find the optimized dimensions, the length and width of substrate were very different from the theoretical results. This proved that although the dimensions can be obtained using theoretical calculations, simulation needs to be done for optimization and more accurate calculation of the dimensions.

F. MPA FABRICATION AND MEASUREMENT

Finally, after simulations were done, MPAs were fabricated using the screen printing method. For FR4 substrate, firing temperature of 200°C was chosen for ferrite thick film due to maximum temperature of which FR4 can withstand. The actual fabricated MPA on FR4 substrate is shown in Fig. 15. As can be seen from the figure, the ferrite layer in between the substrate and the radiating patch is visible from the top view.

Fig. 16 shows the measurement results of MPA with YIG thick film inclusion as substrate overlay on FR4 substrate, labeled as 'Ag + YIG', for frequency ranging from 4 to 7 GHz to analyze the variance or effect of ferrite thick film as substrate overlay at the simulated resonant frequency which is 5.8 GHz. Comparison is also made with antenna without the ferrite thick film, labeled as "Ag only" and with

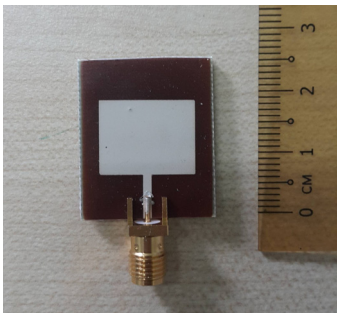

FIGURE 15. The actual fabricated MPA with YIG thick film inclusion as the substrate overlay.

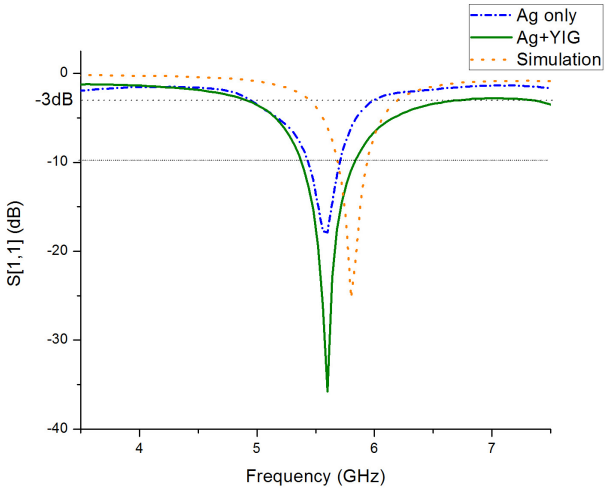

FIGURE 16. VNA Measurement result of MPA with FR4 substrate with YIG thick film inclusion (Ag + YIG), and comparison with MPA without YIG thick film (Ag only) and the simulated result.

the simulation results. Summary of all measured results is shown in Table 2. From the results obtained, the fabricated MPA with ferrite thick film inclusion has shown significant improvements in terms of return loss and bandwidth. The return loss improved from −17.86dB (without YIG thick film) to −35.74dB (with YIG thick film), with 100.11% increase, proving that by adding the ferrite thick film layer helped in maximizing the power being radiated from the antenna. The −3dB bandwidth also showed promising result, increased from 1.04GHz to 1.80GHz, which is 73.07% higher than MPA without ferrite thick film, while −10dB bandwidth which indicates the working frequency when only 10% power is being reflected, also showed increase from 0.26 to 0.40. The results clearly showed that by adding a 20μm-thick ferrite film in MPA fabrication translated to an improved return loss and bandwidth of the patch antenna.

It is noted, however, that there is 200MHz difference at the resonance frequency between the simulated and measured results. While it is the utmost priority to achieve the most accurate results between simulation and fabricated antennas, there are few factors which are difficult to control when fabrications are done in laboratory using semi-automatic screen

TABLE 2. Summary of measured return loss and bandwidth of fabricated MPAs.

Parameter	Ag only (Simulation)	Ag only (Measurement)	Ag + YIG (Measurement)
Resonant frequency, fr (GHz)	5.8	5.6	5.6
Return loss, S11 (dB)	-25.255	-17.86	-35.74
-3dB Bandwidth (GHz)	0.76	1.04	1.80
-10dB Bandwidth (GHz)	0.26	0.26	0.40

TABLE 3. Summary of other parameters of fabricated MPAs.

Parameter	Ag only (Simulation)	Ag only (Measurement)	Ag + YIG (Measurement)
Gain, dB	2.351	2.116	2.406
Radiation efficiency, dB (%)	-3.655 (43.1%)	-3.716 (42.5%)	-3.457 (45.1%)
Total efficiency, dB (%)	-4.036 (39.5%)	-4.111 (38.8%)	-3.813 (41.5%)

printer, such as thickness of the thick film printed onto the substrate, and also the actual dimensions of the fabricated MPA. The properties of the silver patch also may differ from the data in CST material library, which can give effect to the simulation results. Therefore, it can be expected that by improving fabrication methods and the conductive materials used, the frequency difference can be improved further.

Meanwhile, other parameters such as gain, radiation efficiency and total antenna efficiency also have shown some improvements, although not as significant as the return loss and bandwidth of MPA. The other parameters of MPAs are summarized in Table 3.

The closest explanation on the theory of our work is the analysis carried out by Yang *et al.* [27]. According to their work and analysis, magnetic films can give options of having lower μ_r compared to bulk materials, and FMR frequency higher than bulk ferrites based on Snoek limit. Although their work involved the use of 2 μm-thick ferrite thin film deposited on substrate using spin-spray deposition process, the results seem similar to the results obtained by this project.

Ferrite bulks can be imagined as a uniformly spread magnetic sphere, therefore the relative permeability can be described as

$$\mu_r = \frac{4\pi M_s}{H_{net}} + 1 \tag{5}$$

Where $4\pi M_s$ is the saturation magnetization, and H_{net} is the net magnetic field intensity. Angular frequency which is also

the FMR frequency can be determined as

$$\omega_0 = \mu_0 \gamma M_s \tag{6}$$

Where γ is the gyromagnetic ratio. From these two equations, we can rewrite FMR as

$$f_{FMR} \cdot (\mu_r - 1) = \gamma \cdot 4\pi M_s \tag{7}$$

For magnetic films, since they are normally in the xy-plane, we can consider a strong demagnetization field along the z-direction. Therefore, the FMR frequency is increased to be

$$f_{FMR} = \gamma \sqrt{H_{net} \cdot (4\pi M_s + H_{net})} = \gamma H_{net} \sqrt{\mu_r} \tag{8}$$

This shows that the FMR frequency is increased $\sqrt{\mu_r}$ as compared to magnetic spheres, making the ferrite films able to work in gigahertz frequency range.

The effective permeability also plays important role in performance enhancement of the MPA. With increased effective permeability in the MPA structure leads to decrease of characteristic impedance, Z_0 of the substrate. The conductive patch of MPA lies in between free space and the substrate. Therefore, the impedance seen from the patch antenna's view is the parallel combination of both Z_0 from free space and the substrate itself. The radiating patch generally becomes like a generator with two loads in parallel, thus the power split is proportional to the ratio of Z_0. To get more power being delivered or radiated to the free space, either permittivity or the permeability of the substrate can be increased. If the permittivity is increased, in return there are consequences, for example increased surface wave excitations, which makes increasing the permittivity is quite difficult. Therefore another alternative is to increase the permeability of the substrate, which can be done just by depositing thin or thick ferrite films to the originally used substrate to increase the permeability, hence improving the overall performance of the MPA.

VI. CONCLUSION

In conclusion, the addition of YIG thick film layer to MPA device on any substrate can help in improving the performance of MPA itself with size miniaturization. The fabrication process of MPA with YIG thick film as substrate overlay is using low cost, simple screen printing technique, which has proven to be suitable for MPA fabrication on any chosen substrate. Furthermore, the successful fabrication of MPA by utilizing screen printing method of thick film technology opens up possibility to demonstrate ferrite thick film MPA fabrication on flexible substrate of which is hypothesized to show good results to help improve performance of MPA while introducing flexibility to the MPA device, which can have vast applications in future which needs flexible devices along with possibility of reduced size.

ACKNOWLEDGMENT

The authors wish to thank students from Electron Devices group, Functional Devices Laboratory and also staffs and students from Institute of Advanced Technology (ITMA), UPM in the support and help given throughout the commencement of this project.

REFERENCES

[1] D. D. Grieg and H. F. Engelmann, "Microstrip—A new transmission technique for the kilomegacycle range," *Proc. IRE*, vol. 40, no. 12, pp. 1644–1650, 1952.
[2] M. Elhefnawy and W. Ismail, "A microstrip antenna array for indoor wireless dynamic environments," *IEEE Trans. Antennas Propag.*, vol. 57, no. 12, pp. 3998–4002, Dec. 2009.
[3] D. Guha and Y. M. M. Antar, *Microstrip and Printed Antennas: New Trends, Techniques and Applications*. West Sussex, U.K.: Wiley, 2010.
[4] C. A. Balanis, *Antenna Theory: Analysis and Design*, 3rd ed. Hoboken, NJ, USA: Wiley, 2012.
[5] I. Garg, P. Bhartia, and I. J. Bahl, *Microstrip Antenna Design Handbook*. Norwood, MA, USA: Artech House, 2000.
[6] E. Schloemann, "Advances in ferrite microwave materials and devices," *J. Magn. Magn. Mater.*, vol. 209, pp. 15–20, Feb. 2000.
[7] R. K. Mishra, S. S. Pattnaik, and N. Das, "Tuning of microstrip antenna on ferrite substrate," *IEEE Trans. Antennas Propag.*, vol. 41, no. 2, pp. 230–233, Feb. 1993.
[8] G.-M. Yang *et al.*, "Tunable miniaturized patch antennas with self-biased multilayer magnetic films," *IEEE Trans. Antennas Propag.*, vol. 57, no. 7, pp. 2190–2193, Jul. 2009.
[9] P. J. Rainville and F. J. Harackiewicz, "Magnetic tuning of a microstrip patch antenna fabricated on a ferrite film," *IEEE Microw. Guided Wave Lett.*, vol. 2, no. 12, pp. 483–485, Dec. 1992.
[10] K. Borah, A. Phukan, and N. S. Bhattacharyya, "Influence of external magnetic biasing on rectangular patch antenna designed on nano-Co/Ni Fe_2O_4 magnetodielectric substrates," *Proc. SPIE*, vol. 8760, p. 876018, Jan. 2013. [Online]. Available: https://www.spiedigitallibrary.org/conference-proceedings-of-spie/8760/876018/Influence-of-external-magnetic-biasing-on-rectangular-patch-antenna-designed/10.1117/12.2012128.short?SSO=1
[11] E. Andreou, T. Zervos, E. Varouti, A. A. Alexandridis, F. Lazarakis, and G. Fikioris, "A reconfigurable patch antenna printed on YIG-epoxy composite substrate," in *Proc. 10th Eur. Conf. Antennas Propag. (EuCAP)*, Apr. 2016.
[12] A. S. Mekki, M. N. Hamidon, S. M. Yousif, A. Ismail, and I. H. Hasan, "New method to estimate the permittivity of dielectric materials using MSPS," *J. Supercond. Novel Magn.*, vol. 30, no. 12, pp. 3577–3580, 2016.
[13] M. Nelo, A. K. Sowpati, V. K. Palukuru, J. Juuti, and H. Jantunen, "Utilization of screen printed low curing temperature cobalt nanoparticle ink for miniaturization of patch antennas," *Prog. Electromagn. Res.*, vol. 127, pp. 427–444, Mar. 2012.
[14] P. M. T. Ikonen, K. N. Rozanov, A. V. Osipov, P. Alitalo, and S. A. Tretyakov, "Magnetodielectric substrates in antenna miniaturization: Potential and limitations," *IEEE Trans. Antennas. Propag.*, vol. 54, no. 11, pp. 3391–3399, Nov. 2006.
[15] Ü. Özgür, Y. Alivov, and H. Morkoç, "Microwave ferrites, part 1: Fundamental properties," *J. Mater. Sci., Mater. Electron.*, vol. 20, no. 9, pp. 789–834, 2009.
[16] R. Nazlan, M. Hashim, I. R. Ibrahim, and I. Ismail, "Dependence of magnetic hysteresis on evolving single-sample sintering in fine-grained yttrium iron garnet," *J. Supercond. Novel Magn.*, vol. 27, no. 2, pp. 631–639, Aug. 2013.
[17] M. H. S. Abadi, "Development of nanocrystalline thick film gas sensors," Ph.D. dissertation, Faculty Eng., Univ. Putra Malaysia, Kembangan, Malaysia, 2010.
[18] I. H. Hasan, M. N. Hamidon, I. Ismail, R. Osman, and S. Azhari, "Printability and structural analysis of Yttrium iron garnet thick film with low firing temperature," in *Proc. IEEE Regional Symp. Micro Nano Electron. (RSM)*, Aug. 2015, pp. 1–4.
[19] H.-W. Lin, C.-P. Chang, W.-H. Hwu, and M.-D. Ger, "The rheological behaviors of screen-printing pastes," *J. Mater. Process. Technol.*, vol. 197, nos. 1–3, pp. 284–291, Feb. 2008.
[20] A. Verma, A. K. Saxena, and D. C. Dube, "Microwave permittivity and permeability of ferrite–polymer thick films," *J. Magn. Magn. Mater.*, vol. 263, nos. 1–2, pp. 228–234, 2003.
[21] A. Sharma and M. N. Afsar, "Microwave complex permeability and permittivity measurements of commercially available nano-ferrites," *IEEE Trans. Magn.*, vol. 47, no. 2, pp. 308–312, Feb. 2011.

[22] A. Sharma and M. N. Afsar, "Microwave complex permeability and permittivity of nanoferrites," *J. Appl. Phys.*, vol. 109, no. 7, p. 07A503, 2010.
[23] L. Sirdeshmukh, K. K. Kumar, S. B. Laxman, A. R. Krishna, and G. Sathaiah, "Dielectric properties and electrical conduction in yttrium iron garnet (YIG)," *Bull. Mater. Sci.*, vol. 21, no. 3, pp. 219–226, 1988.
[24] R. Nazlan *et al.*, "Compositional and frequency dependent-magnetic and microwave characteristics of indium substituted yttrium iron garnet," *J. Mater. Sci., Mater. Electron.*, vol. 28, no. 3, pp. 3029–3041, 2017.
[25] P. S. Nakar, "Design of a compact microstrip patch antenna for use in wireless/cellular devices," Ph.D. dissertation, Dept. Elect. Eng., Florida State Univ., Tallahassee, FL, USA, 2004.
[26] G. M. Yang *et al.*, "Loading effects of self-biased magnetic films on patch antennas with substrate/superstrate sandwich structure," *IET Microw., Antennas Propag.*, vol. 4, no. 9, pp. 1172–1181, 2010.

INTAN HELINA HASAN (M'13) was born in Kent, U.K., in 1981. She received the bachelor's degree in electrical and computer engineering from Yokohama National University, Kanagawa, Japan, in 2005, the M.Sc. degree in intelligent systems and robotics engineering from Universiti Putra Malaysia, Seri Kembangan, Malaysia, in 2014, where she is currently pursuing the Ph.D. degree in sensor technology.

From 2005 to 2009, she was a Software Engineer with Alps Electric (Malaysia) Sdn Bhd., Nilai, Malaysia. Since 2009, she has been a Research Officer with the Institute of Advanced Technology, Universiti Putra Malaysia. Her research interests include thick-film technology in electron devices, which includes printed electronics, gas sensors, and patch antennas.

MOHD NIZAR HAMIDON (M'05–SM'16) received the B.Sc. degree in physics from the Universiti Malaya, Kuala Lumpur, Malaysia, in 1995, the M.S. degree in microelectronics from the Universiti Kebangsaan Malaysia in 2001, and the Ph.D. degree in wireless sensor from the University of Southampton, Southampton, U.K., in 2005.

From 1995 to 2000, he was a Matriculation Lecturer with Universiti Putra Malaysia, and where he was a tutor from 2001 to 2005. From 2005 to 2011, he was a Lecturer with Faculty of Engineering, Universiti Putra Malaysia, where he has been an Associate Professor since 2011. He has authored over 100 articles and over 50 proceedings. His research interests include packaging, fabrication, data analysis and design for passive wireless applications, thick-film gas sensors fabrication, SAW resonator fabrication for high-temperature wireless applications, design and fabrication of MEMS capacitor for passive wireless sensor applications, and packaging techniques for SAW resonators.

ALYANI ISMAIL (M'06) received the B.Eng. degree (Hons.) in electronic and information engineering from the University of Huddersfield, U.K., in 1999, the M.Sc. degree in communication, computer- and human-centered systems engineering and the Ph.D. degree in electronics engineering majoring in micromachined microwave devices from the University of Wales, U.K., in 2001 and 2006, respectively.

From 2006 to 2011, she was a Lecturer with the Faculty of Engineering, Universiti Putra Malaysia, where she has been an Associate Professor since 2011. She has authored over 200 articles and over 50 proceedings. Her research interest specializes in the development of microwave devices particularly passive filters and antennas, dielectric properties of materials for RF/microwave applications, and engineering education.

ISMAYADI ISMAIL received the B.Sc. degree (Hons.) in materials sciences from Universiti Kebangsaan Malaysia, Bangi, Malaysia, in 2001, and the M.Sc. degree in nanomaterials and the Ph.D. degree in magnetic materials from Universiti Putra Malaysia, Seri Kembangan, Malaysia, in 2007 and 2012, respectively.

From 2002 to 2008, he was a Science Officer with Universiti Putra Malaysia, where he has been a Research Officer with the Institute of Advanced Technology since 2008. His research interests include magnetic materials, nanomaterials, and carbon-based materials, including carbon nanotubes (CNT), graphene, graphene nanoribbons, and CNT cottons from waste cooking oil.

ANWER SABAH MEKKI received the B.Sc. degree in electronic and communication engineering from the University of Technology, Baghdad, Iraq, in 1992, and the Ph.D. degree in sensor technology from Universiti Putra Malaysia, Seri Kembangan, Malaysia, in 2016.

He worked in private sector in designing electronic circuits for wireless control systems, maintenance the computer numerical control machines, and designing the infrared sensors for radar applications. He is currently a Consultant Engineer with Iraqi Engineers Union. His research interests include sensor circuits and microstrip techniques. He is a member of IEICE.

MUHAMMAD ASNAWI MOHD KUSAIMI received the B.Sc. degree in physics from Universiti Putra Malaysia, Seri Kembangan, Malaysia, in 2015, where he is currently pursuing the M.Sc. degree in sensor technology.

His research interests include printed electronics, carbon-based materials for electron devices, and carbon-based ultra-conductor.

SAMAN AZHARI received the B.Sc. degree in materials science from UCSI University, Malaysia, in 2012, and the M.Sc. degree in nanotechnology from Universiti Putra Malaysia, Seri Kembangan, Malaysia, in 2016, where he is currently pursuing the Ph.D. degree in nanotechnology.

His research interests include CNT-PDMS for pressure sensor application, synthesis of CNT and graphene, and synthesis and characterization of TiO_2.

ROSIAH OSMAN (M'13) received the B.Sc. degree in electrical and electronic engineering from the University of Southwestern Louisiana, Lafayette, in 1998, and the M.Sc. degree in intelligent systems and robotics engineering from Universiti Putra Malaysia, Seri Kembangan, Malaysia, in 2015.

From 1999 to 2008, she was a Science Officer with Universiti Putra Malaysia. Since 2008, she has been a Research Officer with the Institute of Advanced Technology, Universiti Putra Malaysia. Her research interests include energy harvesting devices, piezoresistive materials using rice husks, and RFID technology.